

Floquet Topological Phases in One-Dimensional Nonlinear Photonic Crystals

Jian Lu¹, Li He, Zachariah Addison¹, Eugene J. Mele¹, and Bo Zhen^{1*}

Department of Physics and Astronomy, University of Pennsylvania, Philadelphia, Pennsylvania 19104, USA



(Received 18 July 2020; accepted 28 January 2021; published 15 March 2021)

We report on a theoretical analysis of the Floquet topological crystalline phases in driven one-dimensional photonic crystals mediated by second-order optical nonlinearity. We define the photonic Berry connection and photonic polarization in such systems using different methods and prove their equivalence. We present two examples of topological phase transitions in which two Floquet bands cross and open new gaps under the driving field. Finally, we analyze the physical consequences of each topological phase transition by examining edge states and filling anomalies. Our study presents routes toward the realization of robust reconfigurable photonic cavities with topologically protected light confinement.

DOI: [10.1103/PhysRevLett.126.113901](https://doi.org/10.1103/PhysRevLett.126.113901)

Photonic topological phases are classes of solutions to Maxwell's equations that can support robust boundary states protected by the topology of the system's bulk band structure [1–3]. The interplay between the existence of states at the system's boundary and the existence of nontrivial topology in the bulk is known as the bulk-edge correspondence [1]. For example, Chern insulators, which exhibit the quantum anomalous Hall effect supporting unidirectional chiral edge modes on their boundaries, have been demonstrated in two-dimensional (2D) photonic crystals (PhCs) [4–6]. Additionally, systems with Weyl points exhibit Fermi arc dispersions on their surfaces, which have been demonstrated in three-dimensional PhCs [7] and photonic lattices [8]. In practice, topological photonic systems are of interest because their robust optical properties can potentially lead to novel devices such as delay lines, isolators, and circulators [1–3] that are resilient to perturbation or fabrication disorder. Most systems studied so far are limited to solutions to Maxwell's equations in static linear media. Not until recently have there been examples of Floquet topological phases in driven nonlinear optical systems [9–11].

Electric polarizations in crystals have been linked to the Berry phase of the electronic ground state, which provides a cornerstone for the modern theory of polarization [12]. For an insulator, the crystalline symmetries of the system can result in discrete values of the electronic polarization each associated with a unique topological crystalline phase [13–15]. For example, in one-dimensional (1D) systems with inversion symmetry, there exist two topologically inequivalent ground states that are distinguished by the quantized bulk polarizations [16]. Nontrivial edge states carrying fractional charges can be found at the interface between these two topologically distinct phases [14]. Similarly, interfaces between photonic systems can also support topological edge states, which may find practical applications. In particular, 1D photonic systems with C_2

symmetry can support localized edge states, just like the electronic topological dipole phase. These edge states confine light and can be used as robust cavities for lasing [17,18] and for enabling strong light-matter interactions [19].

In this Letter, we study the Floquet topological crystalline phases in 1D nonlinear PhCs subject to temporal modulation. We show that topological phase transitions can occur when the gaps between Floquet bands are closed and reopened by an external driving field. Specifically, we start by defining the Berry connection and Zak phase [20,21] under the framework of the Floquet eigenvalue problems of Maxwell's equations. In contrast to the Floquet topological phases in electronic systems [22], which are defined through Hermitian eigenvalue problems, our formulation is defined through generalized non-Hermitian eigenvalue problems. As a consequence, the eigenvalues in these systems are in general complex, and the particle numbers may not be conserved (e.g., the signal and idler photons in an optical parametric amplifier [23]). We can lay out a simple criterion that guarantees our eigenvalues to be real [10], and the bulk-edge correspondence applies. On the other hand, the left and right eigenvectors are no longer related by complex conjugation owing to the non-Hermiticity of the system. Accordingly, the generalized Berry connection needs to be defined in different ways [24]. We demonstrate the equivalence of these definitions in the presence of C_2 symmetry (see Section I of the Supplemental Material [25]). Similar to the Hermitian case, we further show that the Zak phase of the non-Hermitian Floquet bands is quantized in the presence of C_2 symmetry and can be evaluated using the symmetry eigenvalues at high-symmetry points in the Brillouin zone (BZ) [14]. Accordingly, our method to drive topological phase transitions is to invert two Floquet bands with different C_2 indices at the BZ high-symmetry points by engineering the couplings of two Floquet bands through the appropriate optical nonlinearity and driving field.

We show two specific examples of topological phase transitions and demonstrate their physical significance, which resembles the electronic topological dipole phases with nontrivial polarizations. Here, we note that the mode density in photonic systems, defined as the integrated spectral local density of states within a band continuum, is the photonic analog to the charge density within a band in electronic systems [28]. As such, we define the polarization of a photonic band as the first moment of the mode density in the entire band and the filling anomaly as the anomalous depletion or overfilling of the mode densities within the band continuum. The first example engineers the phase transition between a trivial static phase and a polarized Floquet phase, leading to the discovery of systems with new topological edge states as well as filling anomalies with a discrete packet of energy in the confined mode [14,15]. The second example engineers a phase transition between a polarized static phase and an anomalous Floquet phase where we show that new edge states may appear but without filling anomalies. By tuning the system parameters, we find that the anomalous phase may become topologically indistinguishable from a trivial phase, even though no additional gap closing is involved in the parameter tuning process. This highlights one of the major differences between anomalous Floquet phases in our 1D system and 2D Chern insulators [29–31].

We start by formulating the Floquet eigenvalue problem and defining the 1D topological invariants. The nonlinear PhC under study is schematically shown in Fig. 1(a), which consists of alternating layers of a second-order nonlinear material, LiNbO₃, with a linear permittivity of $\epsilon_{xx} = \epsilon_{yy} = 4.97$ and $\epsilon_{zz} = 4.67$, and a linear material, Si, with $\epsilon = 12.25$. Both materials are chosen because they are commonly used in integrated photonics. In the visible and near-infrared regime of interest, LiNbO₃ has a large second-order nonlinear susceptibility of $\chi_{zzz}^{(2)} = 2d_{33} = 62$ pm/V [32], which can lead an appreciable Floquet gap under moderately strong driving fields. The PhC is uniform along the y and z directions and has a periodicity of a along the x direction. The width of the Si layer is $w = 0.6a$. The LiNbO₃ is x cut and the crystallographic c axis is parallel to the z axis as defined in the inset. In this Letter, only transverse-magnetic (TM) modes propagating along the x direction with field components (E_z, H_x, H_y) are considered. The static band structure of the four lowest bands and their corresponding mode profiles are calculated using a finite-element solver with the band structure shown in Fig. 1(b). The Zak phase of a TM band is defined as the integral of the Berry connection over the BZ

$$\theta_{\text{Zak}} = \int_{\text{BZ}} \mathcal{A}_k dk = i \int_{\text{BZ}} \langle u_k^z | \epsilon_{zz} \partial_k | u_k^z \rangle dk, \quad (1)$$

where \mathcal{A}_k is the Berry connection and $|u_k^z\rangle$ is the E_z component of the Bloch wave function at wave vector

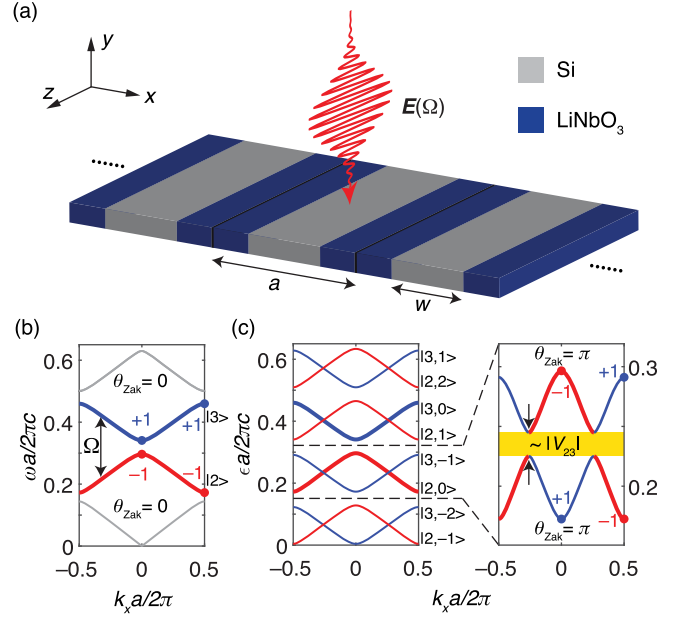


FIG. 1. Floquet topological phase transition in a driven 1D PhC. (a) Schematic of a 1D nonlinear PhC that consists of alternating layers of Si and LiNbO₃. An external driving field $E(\Omega)$ couples different TM modes via the electro-optic effect of LiNbO₃. (b) The dispersion of the four lowest TM bands is calculated. The C_2^y eigenvalues (± 1) of the mode profiles at the BZ center (Γ) and edge (X) are evaluated. The second (red) and third (blue) static bands, both topologically trivial, are coupled via the external driving field. (c) Under the driving field, Floquet bands are created and a band inversion is induced between two Floquet bands, i.e., band $|3, -1\rangle$ and $|2, 0\rangle$ at Γ . After inversion, a Floquet gap is opened (yellow) and both Floquet bands have topologically nontrivial bulk polarizations.

$k = k_x$. In the presence of the C_2^y symmetry, which is the 180° rotation symmetry around the y axis in our structure, the Bloch Hamiltonian obeys $C_2^y \hat{H}_k C_2^{y-1} = \hat{H}_{-k}$. Based on the symmetry operation detailed in Section I of the Supplemental Material [25], the Zak phase is related to the eigenvalues of the C_2^y operator at the center (Γ) and edge (X) of the BZ as [14]

$$e^{i\theta_{\text{Zak}}} = C_2^y(\Gamma) C_2^y(X). \quad (2)$$

As the C_2^y eigenvalues at Γ and X are ± 1 , the Zak phases are quantized as 0 or π , modulo 2π . Accordingly, the polarization of a band, $p_x = \theta_{\text{Zak}}/2\pi$, is quantized to be either 0 (topologically trivial) or 0.5 (nontrivial), modulo 1. For the second (third) band, shown in red (blue), the C_2^y eigenvalues at both Γ and X are -1 ($+1$), meaning the band is topologically trivial with $p_x = 0$.

Next we show how topological phase transitions can be induced by external driving fields in the 1D nonlinear PhCs. A monochromatic driving field $E(\Omega) = E_z^d \cos(\Omega t) \hat{z}$ impinges from the y direction and periodically modulates the permittivity of LiNbO₃ via the electro-optic effect,

$\Delta\epsilon_{zz}(t) = 2\chi_{zzz}^{(2)}E_z^d \cos(\Omega t)$. In contrast to the static system, the driven system only has a discrete translation symmetry in time. Accordingly, each static band $|j\rangle$ is transformed into a set of Floquet bands $|j, m\rangle$ whose frequencies are separated by $m\Omega$ (with m an integer), as shown in Fig. 1(c). The Floquet eigenvalue equation is derived from Maxwell's equations by considering the time-varying permittivity [10] (see Section II of the Supplemental Material [25] for details of the derivation). The Floquet Hamiltonian assumes a tridiagonal form where couplings between adjacent Floquet bands arise from the second-order nonlinearity. Couplings between nonadjacent Floquet bands ($|\Delta m| > 1$) are also possible via higher-order nonlinear optical processes involving more pump photons. Such processes are typically much weaker than the second-order nonlinear processes and are not considered in this Letter. Though their frameworks are similar, the 1D system here and the 2D Floquet-Chern insulator in [10] represent different types of topological phases and are manifested by different physical consequences. For simplicity, we consider the Floquet eigenvalue problem within the sub-space spanned by the second and third static bands only, although more bands can also be taken into account under this framework. Under the rotating wave approximation, the eigenvalue equation that couples two Floquet states $|2, 0\rangle$ and $|3, -1\rangle$ at each k_x is given by

$$\begin{bmatrix} \omega_2 & 0 \\ -\Omega V_{23}^\dagger & \omega_3 - \Omega \end{bmatrix} \begin{bmatrix} c_{2,0} \\ c_{3,-1} \end{bmatrix} = \epsilon \begin{bmatrix} 1 & V_{23} \\ V_{23}^\dagger & 1 \end{bmatrix} \begin{bmatrix} c_{2,0} \\ c_{3,-1} \end{bmatrix}. \quad (3)$$

Here, ϵ is the Floquet eigenvalue, also known as the quasienergy, and $V_{23} = \langle 2, 0 | \chi_{zzz}^{(2)} E_z^d | 3, -1 \rangle / 2$ is the coupling strength between modes on bands $|2, 0\rangle$ and $|3, -1\rangle$ at the same k_x arising from the nonlinearity. Solving Eq. (3) at each k_x yields the quasienergy spectra $\epsilon(k_x)$, as shown in Fig. 1(c). Because of the conservation of photon numbers, the Floquet eigenvalues are always real when ω_2 and ω_3 are both at positive or negative frequencies [10].

A topological phase transition is induced by inverting Floquet bands $|2, 0\rangle$ with $|3, -1\rangle$. For a small driving frequency Ω , Floquet band $|2, 0\rangle$ is always at a lower frequency than $|3, -1\rangle$, separated by a quasienergy gap. As Ω increases to the critical value of $\Omega_c = \omega_3(\Gamma) - \omega_2(\Gamma)$, the Floquet gap is closed at Γ , where the coupling strength V_{23} between the two bands vanishes due to the C_2^y -symmetry mismatch. As Ω further increases, the band inversion is completed, and a new Floquet gap is opened with the gap size proportional to the magnitude of the coupling strength $|V_{23}|$. More importantly, both Floquet bands become topologically nontrivial after the band inversion. The C_2^y indices switch at Γ , and accordingly, the Zak phases of both bands change to π , indicating a nontrivial polarization for each band. This topological phase transition is further confirmed by directly integrating

the Berry connection over the BZ to calculate the Zak phase [33] (see Section II of the Supplemental Material [25] for more details of the calculation).

Next we present the physical consequences of this topological phase transition from a trivial static phase to a nontrivial polarized Floquet phase. Specifically, we show that the driving field induces new edge states accompanied by an anomalous depletion or overfilling of mode densities within the bands, as schematically shown in Fig. 2(a). In the case of the trivial static phase, for a finite system with N unit cells, each bulk band becomes a set of N modes representing the bulk continuum (schematically shown in green). Under the driving field, the bulk bands undergo a transition into the polarized Floquet phase with nontrivial polarizations. As a result, two degenerate topological edge states emerge inside the Floquet gap, marked as red and blue circles. These two edge states have contributions from the bulk states in the bands above and below the gap. Consequently, each bulk continuum is left with only $N - 1$ states, leading to a filling anomaly that is robust against perturbations preserving C_2 symmetry. In comparison,

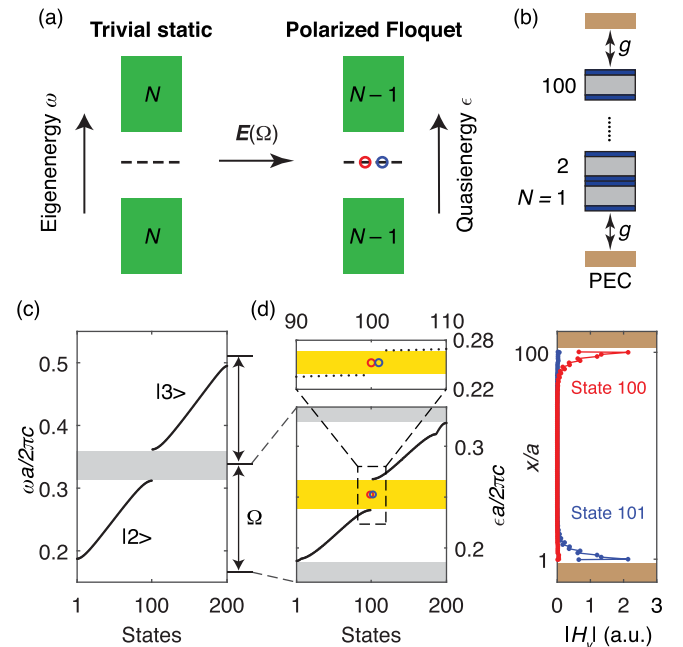


FIG. 2. Trivial static to polarized Floquet phase transition. (a) Schematic drawing of drive-induced edge states (red and blue circles) and filling anomalies that do not exist in the static system. (b) The finite system consists of a PhC with 100 unit cells terminated by PECs, shown in brown. The width of the air gaps g can be modified. (c) Numerical simulation results of the energy spectrum of the trivial static finite system, where both band continua consist of 100 states, corresponding to bands $|2\rangle$ and $|3\rangle$ in Fig. 1(b). (d) Under an external driving field, two edge states (blue and red circles) emerge in the Floquet gap (shaded in yellow) corresponding to states 100 and 101. The mode profiles confirm that these two states are localized at the top and bottom boundaries.

while edge states may also appear in topologically trivial systems by tuning the boundary condition, such edge states have contributions solely from the bulk states below or above the gap, leaving $N - 2$ states in the bulk continuum, and this does not lead to filling anomalies.

We numerically demonstrate the topological edge states and filling anomalies by solving the Floquet eigenvalue problem for a finite PhC that consists of $N = 100$ unit cells, as shown in Fig. 2(b). The unit cell has the same parameters as in Fig. 1(a). The finite PhC is placed between two perfect electric conductors (PECs), which are topologically trivial. Two air gaps with thickness of $g = 0.2a$ are placed between the PhC and PEC. As shown in Fig. 2(c), the energy spectrum of the finite system consists of two bulk continua, each with 100 eigenstates, separated by an energy gap (shaded in gray). These results are consistent with the bands $|2\rangle$ and $|3\rangle$ in Fig. 1(b). All 200 bulk states are mixed under a driving field at the frequency of $\Omega a/2\pi c = 0.1717$. For the ease of presentation, a strong driving field of $E_z^d = 20$ GV/m is used here in our calculation; however, a much lower field below the damage threshold of LiNbO₃ of ~ 1 GV/m [32] is adequate to demonstrate the physical consequences in practice.

The quasienergy spectrum is shown in Fig. 2(d), where a Floquet gap (shaded in yellow) is opened by the driving field. Additionally, two edge states, corresponding to states 100 and 101, appear in this Floquet gap. Accordingly, both bulk continua below and above the Floquet gap contain 99 states, which demonstrates the presence of a drive-induced filling anomaly in our system. The localization of the edge states is confirmed by their mode profiles $|H_y|$, as shown in the right panel. The energy degeneracy between these two edge states is protected by the C_2^y symmetry of the system. Because of the lack of chiral symmetry in Maxwell's equations around this gap frequency, the energy of the two edge states is not pinned at the center of the gap; instead it can be shifted by tuning system parameters such as the air gap width g . However, as long as C_2^y symmetry is preserved, the filling anomaly is always present, even if the two edge states merge into the bulk continuum above or below the gap (see Section III of the Supplemental Material [25] for details).

Next we present a different kind of topological phase transition from a polarized static phase to an anomalous Floquet phase, which is shown schematically in Fig. 3(a). The new unit cell shares the same materials and orientation as the previous one, with the only difference being that the width of the Si is reduced to $w = 0.2a$. (Simulation results of the dispersion of the lowest static TM bands are shown in Section II of the Supplemental Material [25].) The C_2^y indices at Γ and X for the first, second, and third bands are $(+1, +1)$, $(-1, +1)$, and $(+1, -1)$, respectively. Accordingly, the first band is topologically trivial with $p_x = 0$, while the second band ($|2\rangle$) and the third band ($|3\rangle$) have nontrivial polarizations of $p_x = 0.5$. The calculated

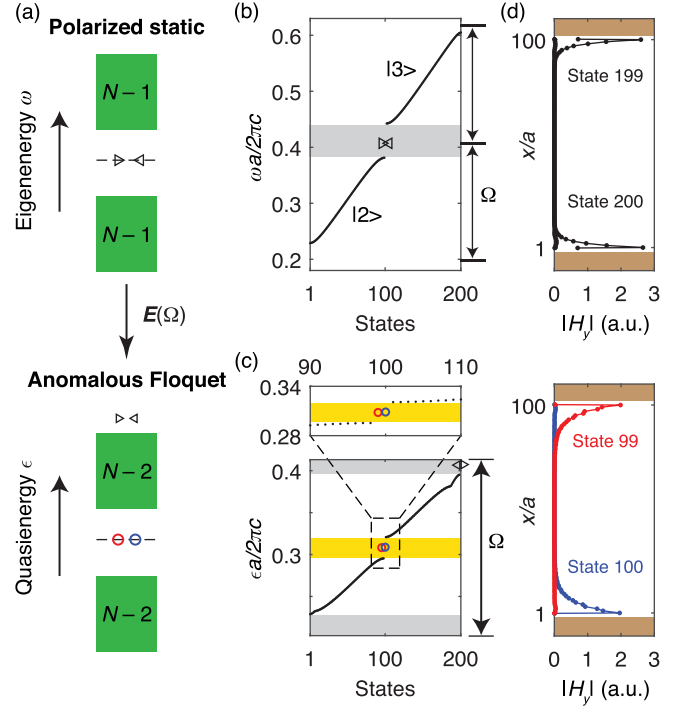


FIG. 3. Polarized static to anomalous Floquet phase transition. (a) Schematic drawings of static edge states (triangles), drive-induced edge states (circles), and energy spectra of the polarized static phase and the anomalous Floquet phase. (b) Numerical simulation results of the energy spectrum of a static finite system with 100 unit cells in the polarized phase, exhibiting edge states (triangles) in the static energy gap (shaded in gray). (c) Under a driving field, two new edge states (red and blue circles), corresponding to states 99 and 100, emerge in the Floquet gap (shaded in yellow), while the static edge states (states 199 and 200), are preserved (triangles). The upper panel shows an enlarged view of the spectrum within the dashed box. (d) Mode profiles of the static edge states (199 and 200), shown in black lines, and drive-induced edge states (99 and 100), shown in red and blue lines, which are all localized at the boundaries.

energy spectrum for a finite system with 100 unit cells is shown in Fig. 3(b). Two edge states appear inside the static energy gap due to the nontrivial polarization below the gap, labeled by the triangles in Fig. 3(b). Under a driving field at the frequency of $\Omega a/2\pi c = 0.2099$, a band inversion is induced between $|2, 0\rangle$ and $|3, -1\rangle$ at Γ . After the band inversion, a Floquet gap is opened by the driving field as shown in the quasienergy spectrum in Fig. 3(c). Judging from the C_2^y indices, both Floquet bands are topologically trivial with $p_x = 0$. However, along with the edge states inherited from the static setting (triangles), this Floquet system exhibits new edge states within the Floquet gap, which are labeled by circles in Fig. 3(c). The localization of static (black lines) and drive-induced edge states (blue and red lines) is confirmed by their mode profiles shown in Fig. 3(d). Similar phenomena have been observed in 2D systems, known as the anomalous Floquet phase [29–31],

which support gapless edge states above and below Floquet bands with zero Chern numbers.

We note that filling anomalies, not edge states, are the key characteristics of topological phases in 1D. Therefore, we further study the 1D anomalous Floquet phase from the filling anomaly point of view and show that it is topologically indistinguishable from a 1D trivial phase. Specifically, we start from the spectrum of the finite PhC in Fig. 3(c), where each Floquet band continuum consists of 98 states. By changing the air gap width g , while maintaining the C_2^y symmetry and keeping bulk energy gaps open, we show that the two pairs of edge states can be merged into the upper and lower continua respectively. After this operation, both Floquet band continua consist of 100 states, which is compatible with the unit cell number and does not show a filling anomaly (see Section III of the Supplemental Material [25] for more details). This is in contrast to the anomalous Floquet phase in 2D where the edge states can only be eliminated by gap closing [31].

To summarize, we analyze the Floquet topological crystalline phases in driven 1D nonlinear PhCs, which are described by generalized non-Hermitian eigenvalue problems. Through the study of two types of topological phase transitions, we elucidate the definition of topological invariants and their physical consequences in these systems. Our formalism can be further generalized to compute quadrupole moments and to study high-order topology in driven nonlinear systems. Our framework is also applicable to other nonlinear systems without particle conservation, such as phonons and polaritons. The presented 1D Floquet topological phases may enable reconfigurable cavities with applications in on-chip Q-switch lasers and light-wave-controlled strong light-matter interactions (see Section V in the Supplemental Material [25] for details).

This work was partly supported by the National Science Foundation through the University of Pennsylvania Materials Research Science and Engineering Center DMR-1720530, the US Office of Naval Research (ONR) Multidisciplinary University Research Initiative (MURI) grant N00014-20-1-2325 on Robust Photonic Materials with High-Order Topological Protection, and the Air Force Office of Scientific Research under award number FA9550-18-1-0133. J. L. was also supported by the Army Research Office under award contract W911NF-19-1-0087. Work by Z. A. and E. M. was supported by the U.S. Department of Energy, Office of Basic Energy Sciences under grant number DE FG02 84ER45118.

*Corresponding author.

bozhen@sas.upenn.edu

[1] L. Lu, J. D. Joannopoulos, and M. Soljačić, Topological photonics, *Nat. Photonics* **8**, 821 (2014).

- [2] T. Ozawa, H. M. Price, A. Amo, N. Goldman, M. Hafezi, L. Lu, M. C. Rechtsman, D. Schuster, J. Simon, O. Zilberberg *et al.*, Topological photonics, *Rev. Mod. Phys.* **91**, 015006 (2019).
- [3] A. B. Khanikaev and G. Shvets, Two-dimensional topological photonics, *Nat. Photonics* **11**, 763 (2017).
- [4] F. D. M. Haldane and S. Raghu, Possible Realization of Directional Optical Waveguides in Photonic Crystals with Broken Time-Reversal Symmetry, *Phys. Rev. Lett.* **100**, 013904 (2008).
- [5] Z. Wang, Y. D. Chong, J. D. Joannopoulos, and M. Soljačić, Reflection-Free One-Way Edge Modes in a Gyromagnetic Photonic Crystal, *Phys. Rev. Lett.* **100**, 013905 (2008).
- [6] Z. Wang, Y. Chong, J. D. Joannopoulos, and M. Soljačić, Observation of unidirectional backscattering-immune topological electromagnetic states, *Nature (London)* **461**, 772 (2009).
- [7] L. Lu, Z. Wang, D. Ye, L. Ran, L. Fu, J. D. Joannopoulos, and M. Soljačić, Experimental observation of Weyl points, *Science* **349**, 622 (2015).
- [8] J. Noh, S. Huang, D. Leykam, Y. D. Chong, K. P. Chen, and M. C. Rechtsman, Experimental observation of optical Weyl points and Fermi arc-like surface states, *Nat. Phys.* **13**, 611 (2017).
- [9] V. Peano, M. Houde, C. Brendel, F. Marquardt, and A. A. Clerk, Topological phase transitions and chiral inelastic transport induced by the squeezing of light, *Nat. Commun.* **7**, 10779 (2016).
- [10] L. He, Z. Addison, J. Jin, E. J. Mele, S. G. Johnson, and B. Zhen, Floquet Chern insulators of light, *Nat. Commun.* **10**, 4194 (2019).
- [11] K. Fang and Y. Wang, Anomalous Quantum Hall Effect of Light in Bloch-Wave Modulated Photonic Crystals, *Phys. Rev. Lett.* **122**, 233904 (2019).
- [12] R. D. King-Smith and D. Vanderbilt, Theory of polarization of crystalline solids, *Phys. Rev. B* **47**, 1651 (1993).
- [13] W. A. Benalcazar, B. A. Bernevig, and T. L. Hughes, Quantized electric multipole insulators, *Science* **357**, 61 (2017).
- [14] W. A. Benalcazar, B. A. Bernevig, and T. L. Hughes, Electric multipole moments, topological multipole moment pumping, and chiral hinge states in crystalline insulators, *Phys. Rev. B* **96**, 245115 (2017).
- [15] W. A. Benalcazar, T. Li, and T. L. Hughes, Quantization of fractional corner charge in C_n -symmetric higher-order topological crystalline insulators, *Phys. Rev. B* **99**, 245151 (2019).
- [16] W. P. Su, J. R. Schrieffer, and A. J. Heeger, Solitons in Polyacetylene, *Phys. Rev. Lett.* **42**, 1698 (1979).
- [17] P. St-Jean, V. Goblot, E. Galopin, A. Lemaître, T. Ozawa, L. Le Gratiet, I. Sagnes, J. Bloch, and A. Amo, Lasing in topological edge states of a one-dimensional lattice, *Nat. Photonics* **11**, 651 (2017).
- [18] Y. Ota, R. Katsumi, K. Watanabe, S. Iwamoto, and Y. Arakawa, Topological photonic crystal nanocavity laser, *Commun. Phys.* **1**, 86 (2018).
- [19] T. Karzig, C.-E. Bardyn, N. H. Lindner, and G. Refael, Topological Polaritons, *Phys. Rev. X* **5**, 031001 (2015).
- [20] J. Zak, Berry's Phase for Energy Bands in Solids, *Phys. Rev. Lett.* **62**, 2747 (1989).

- [21] M. Xiao, Z. Zhang, and C. T. Chan, Surface Impedance and Bulk Band Geometric Phases in One-Dimensional Systems, *Phys. Rev. X* **4**, 021017 (2014).
- [22] N. H. Lindner, G. Refael, and V. Galitski, Floquet topological insulator in semiconductor quantum wells, *Nat. Phys.* **7**, 490 (2011).
- [23] R. W. Boyd, *Nonlinear Optics* (Academic Press, New York, 2019).
- [24] H. Shen, B. Zhen, and L. Fu, Topological Band Theory for Non-Hermitian Hamiltonians, *Phys. Rev. Lett.* **120**, 146402 (2018).
- [25] See Supplemental Material, which includes Refs. [26,27], at <http://link.aps.org/supplemental/10.1103/PhysRevLett.126.113901> for details of the derivations and supporting data including topological invariants in non-Hermitian systems with C_2 symmetry, Floquet eigenvalue problems of driven nonlinear PhCs, the physical consequences of merging edge states with bulk continua, a summary of key parameters in 1D Floquet topological phases, and the applications of 1D Floquet topological phases.
- [26] J. N. Winn, S. Fan, J. D. Joannopoulos, and E. P. Ippen, Interband transitions in photonic crystals, *Phys. Rev. B* **59**, 1551 (1999).
- [27] A. Faraon, I. Fushman, D. Englund, N. Stoltz, P. Petroff, and J. Vučković, Coherent generation of non-classical light on a chip via photon-induced tunnelling and blockade, *Nat. Phys.* **4**, 859 (2008).
- [28] C. W. Peterson, T. Li, W. A. Benalcazar, T. L. Hughes, and G. Bahl, A fractional corner anomaly reveals higher-order topology, *Science* **368**, 1114 (2020).
- [29] M. S. Rudner, N. H. Lindner, E. Berg, and M. Levin, Anomalous Edge States and the Bulk-Edge Correspondence for Periodically Driven Two-Dimensional Systems, *Phys. Rev. X* **3**, 031005 (2013).
- [30] L. J. Maczewsky, J. M. Zeuner, S. Nolte, and A. Szameit, Observation of photonic anomalous Floquet topological insulators, *Nat. Commun.* **8**, 13756 (2017).
- [31] M. S. Rudner and N. H. Lindner, Band structure engineering and non-equilibrium dynamics in Floquet topological insulators, *Nat. Rev. Phys.* **2**, 229 (2020).
- [32] R. L. Sutherland, *Handbook of Nonlinear Optics* (CRC Press, Boca Raton, FL, 2003).
- [33] T. Fukui, Y. Hatsugai, and H. Suzuki, Chern numbers in discretized Brillouin zone: Efficient method of computing (spin) hall conductances, *J Phys. Soc. Jpn.* **74**, 1674 (2005).